

Article citation info:

Wang H, Zhang Z, Li J, Xin W, Han C, Fault analysis and reliability evaluation for motorized spindle of cycloidal gear grinding machine based on multi-source bayes, *Eksploatacja i Niezawodność – Maintenance and Reliability* 2024: 26(1) <http://doi.org/10.17531/ein/175010>

Fault analysis and reliability evaluation for motorized spindle of cycloidal gear grinding machine based on multi-source bayes

Indexed by:



Huiliang Wang^{a,b*}, Zhijie Zhang^a, Jie Li^c, Wen Xin^b, Chunyang Han^b

^a School of Mechatronics Engineering, Henan University of Science and Technology, Luoyang, Henan Province, China

^b State Key Laboratory of Intelligent Mining Heavy Equipment, Luoyang, Henan Province, China

^c AVIC Jonhon Optron Technology Co., Ltd., Luoyang, Henan Province, China

Highlights

- A Monte Carlo simulation method based on multi-source Bayes is proposed to establish the fuzzy fault tree model of motorized spindles.
- Using a fault tree as the simulation model, the feasibility of reliability simulation is verified by comparing fuzzy importance with simulation importance.
- The wavelet packet transform is combined with empirical mode decomposition to extract faults and simulate equipment reliability.

Abstract

A Monte Carlo simulation method based on multisource bayes is proposed to improve the reliability of motorized spindles in cycloid gear grinding machines and reduce their failure rate. Based on field investigations and motorized spindle maintenance records, a fault tree model of a motorized spindle was established, and the fuzzy importance of each bottom event was evaluated. The fault tree of a motorized spindle was used as a Monte Carlo reliability simulation model, and its importance was used as the input parameter for the simulation. The reliability evaluation index of the motorized spindle was obtained at different simulation times. The feasibility and accuracy of the reliability simulation were verified by comparing the importance and simulation importance. A vibration test was designed for bearing faults with high importance, and fault extraction was performed by combining the wavelet packet transform and empirical mode decomposition. This method can also be used to simulate and analyze the reliability of other equipment or machine tools.

Keywords

motorized spindle, cycloidal gear grinding machine, Monte Carlo simulation, reliability evaluation, multi-source bayes

This is an open access article under the CC BY license (<https://creativecommons.org/licenses/by/4.0/>)

1. Introduction

With the rapid development of various industries and the continuous advancement of manufacturing technology, the demand for various products, such as machinery and transport tools, continues to increase, which has accelerated the research and development of computer numerical control (CNC) machine tools. As key equipment in the precision machining stage of gears, cycloidal gear grinding machines will become mainstream in the development of high-end gear grinding

machines in the future, owing to their unique advantages. A cycloidal gear grinding machine primarily comprises three linear motion axes and a rotary axis.

As key components, motorized spindles are of great significance in the development of cycloid gear grinding machines. The motorized spindle operates under working conditions of high speed, high power, and high load, which makes its parts more prone to fatigue, fracture, and other faults.

(*) Corresponding author.

E-mail addresses:

H. Wang (ORCID: 0000-0001-8456-4345) whl-ly@163.com, Z. Zhang 1184528366@qq.com, J. Li 614937994@qq.com, W. Xin xinwen@citic-hic.com.cn, C. Han hancy@citic-hic.com.cn

Failure directly affects the machining performance of the machine tool, increasing the failure rates of parts. Therefore, to ensure the reliability and machining accuracy of the cycloid gear grinding machine, it is important to analyze and evaluate the failure of the motorized spindle and formulate corresponding maintenance and repair strategies to improve its reliability of the motorized spindle.

In the reliability analysis of machine tools, the determination of the fault distribution model of an entire machine system is the basis for subsequent research. To solve the limitations of the failure-mode effect and criticality analysis, Nilesh [1] proposed a multi-factor decision-making method based on the Complex Proportional Assessment Grey (COPRAS-G) method. Gajanand [2] considered the fuzzy Failure Mode, Effects and Criticality Analysis (FMECA) method to be more suitable for the system criticality problem by comparing traditional and fuzzy FMECA analysis methods. Lee [3] analyzed the fault in a gear pump and explored an intelligent wear detection process based on the Mel-Frequency Cepstrum coefficient. Joanna [4] proposed and discussed a matrix FMEA analysis method and applied it to select hydraulic components. Soltanali [5] proposed a fuzzy fault tree. The fault probability of the model is predicted using the active technology of knowledge to formulate a convenient maintenance plan for the equipment.

Reliability modeling predicts, analyses, and evaluates the reliability of a system at different times by establishing a reliable model. Qian [6] proposed a Monte Carlo simulation method to study the influence of random crane movement considering radiation effect on the reliability of rail beam structure. Wang [7] proposed a fast reliability evaluation method for backup redundant systems based on survival signature. Zhu [8] proposed a reliability probabilistic modeling method based on Markov model and subset simulation to solve the reliability problem of wind turbine long-term fatigue. On the basis of zero failure data lifetime reliability evaluation method, Chen [9] proposed a reliability evaluation method and simulation test method which fused numerical simulation with zero failure data. The prediction accuracy of aero-engine compressor disc life is improved. Yu [10] proposed a numerical analysis method based on computer simulation and Monte Carlo method to solve the problem of reliability life prediction of power systems composed of units with different life

distributions. Denkena [11] proposed a hierarchical Bayesian change-point regression model to estimate the distribution type of fault time and constructed a parameter estimation method based on the Gibbs sampling algorithm. Siju [12] combined a parameter degradation model and a Bayesian method to evaluate the reliability of components. Yalcinkaya [13] used the Bayes method to estimate the parameter interval for small-sample problems and then verified the effectiveness of this method by simulation. Wang [14] proposed a small-sample fault data reliability modeling method based on the Bootstrap–Bayes method, which improved the reliability of cycloidal grinding machines, reduced the machine failure rate, and shortened the maintenance time. Maskura [15] proposed a reliability growth model with a bathtub fault detection rate and compared it with a classical model. The results demonstrate its advantages in terms of reliability prediction.

Reliability simulation refers to the process of completing reliability analysis using simulation technology. Huang [16] simulated the reliability of repaired mechanical equipment based on the failure time density function of parts and reevaluated the reliability of the equipment, which is of great significance for the later formulation of the corresponding maintenance strategy. Hoseinie [17] used the Kamat–Riley Monte Carlo simulation method to simulate the reliability of a shearer water system and completed a reliability evaluation of the system according to the obtained reliability curve. Li [18] combined a reliability growth coefficient with a Monte Carlo simulation model to predict the reliability of a spinning machine. Xiao [19] proposes an efficient reliability method based on adaptive agent model, which solves the problem that the existing reliability methods of adaptive sequence sampling are limited to Kriging model and Monte Carlo simulation reliability methods based on Kriging model produce random results without considering the uncertainty of initial samples. Sun [20] proposes a reliability analysis method based on Kriging model combined with least improvement function (LIF), Markov Chain Monte Carlo and Monte Carlo simulations to deal with nonlinear performance functions, small probabilities, complex limit states and high-dimensional engineering problems.

Fault detection refers to determining whether a fault exists in the product through detection and testing, and fault diagnosis is used to locate the fault on this basis. Currently, the main

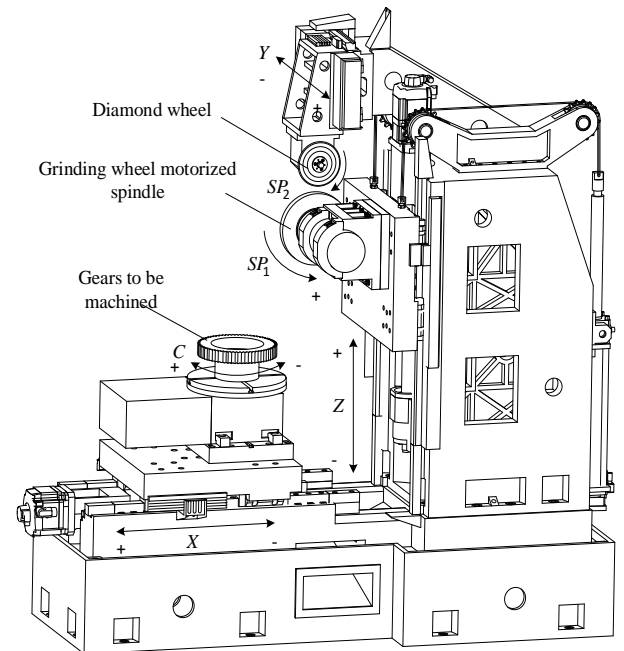
research directions are model-based fault detection and diagnosis, data-based fault detection and diagnosis, and deep learning-based fault detection and diagnosis [21-23]. Mathur [24] used Variational Modal Decomposition (VMD), Empirical Mode Decomposition (EMD), and Ensemble Empirical Mode Decomposition (EEMD) to detect faults in rolling bearings and then used the k-nearest neighbor, Support Vector Machine (SVM), and naive Bayesian classifier to classify the faults and compare their accuracies. Talhaoui [25] proposed a method to diagnose the broken-bar fault of an induction motor rotor using fuzzy logic technology and detected, identified, and predicted the fault of the machine in the running state using wavelet packet decomposition. Lundgren [26] proposed a data-driven fault classification algorithm to deal with imbalanced datasets, class overlap, and unknown faults and evaluated the practicability of this method. Wang [27] performed finite element modal analysis on a rotary vector (RV) reducer, determined the frequency distribution and deformation of each order of the component by analyzing the frequency and arrangement distribution of the component, and established a transmission performance test platform for the RV reducer, which improved its transmission characteristics.

According to current research trends, reliability research on CNC machine tools and their key components is mainly based on system engineering, including fault analysis, reliability modeling and evaluation, reliability simulation, and fault diagnosis. However, in reliability simulation technology, there are few studies on the failure distribution of failure modes, and most are simplified by an exponential distribution. In fault detection, it is difficult to obtain a characteristic fault signal owing to noise interference or other factors. Therefore, this study investigates the fault analysis and reliability evaluation of the motorized spindle of a cycloid gear grinding machine using various methods and provides new ideas and references for the development of reliability technology.

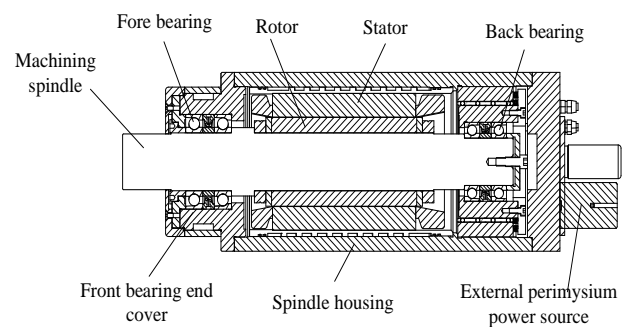
2. Fault analysis and reliability evaluation of motorized spindle

Various types of faults may occur during the operation of the motorized spindle of a cycloid gear grinding machine. It is necessary to analyze the faults of the motorized spindle to improve the average trouble-free working time and equipment

level. By analyzing the reasons that may lead to equipment failure, a maintenance and repair plan is formulated in advance, the hidden danger of failure is eliminated, and the fault-free working time of the equipment is prolonged to improve its reliability. This section analyzes the fuzzy fault tree of a motorized spindle and studies the key factors leading to its failure of the motorized spindle. A structural diagram is shown in Figure 1. The mechanical structure, which is composed of a ball screw and ball guide rail, is responsible for the feed in the X-, Y-, and Z-directions. The grinding wheel, motorized spindle, and diamond grinding wheel are responsible for the modification and processing of the cycloidal gear. The grating and grating ruler is responsible for the closed-loop control of the cycloid gear grinding machine for achieving high-precision control of the cycloidal gear.



a) Cycloidal gear grinding machine.



b) Motorized spindle.

Fig. 1. Structure and motion axis diagram of cycloidal gear grinding machine.

A. MOTORIZED spindle fault data acquisition

Reliability data reflect the working conditions of the equipment, which is of great significance for fault analysis and reliability research [28,29]. According to the source of the fault data, they can be roughly divided into reliability test data, trial operation data, and maintenance data. Reliability test data are generally obtained from life tests, which are characterized by high costs and small sample sizes. The trial operation data are obtained

from the trial operation fault record, which is prone to early failure, and the maintenance data are obtained from the maintenance station fault record, which has the characteristics of multiple source fault types. In this study, maintenance records were selected as reliability data, and the fault maintenance records of a motorized spindle production company were collected. The fault records of motorized spindle are shown in table 1.

Table 1. Fault records of motorized spindle.

Model	Numbering	Turn the shaft	Strike	Motor	Bearing	Leaking	Precision
Model 1	2022-007-083	Difficulty turning	No	Normal	Damage	No	Inner diameter runout 5
	2022-007-121	Rotatable	Yes	Normal	Damage	No	Inner diameter runout 3
	2022-004-037	Difficulty turning	No	Normal	Damage	No	Inner diameter runout 3
	2022-004-034	Difficulty turning	No	Normal	Damage	No	Inner diameter runout 3
Model 2	2022-004-015	Rotatable	No	Normal	Damage	No	Inner diameter runout 3
	2015-012-020	Rotatable	No	Normal	Damage	No	Inner diameter runout 5
	2015-011-045	Unable to turn	No	Damage	Damage	No	Inner diameter runout 4
Model 3	2015-012-020	Rotatable	No	Normal	Damage	No	Inner diameter runout 3
Model 4	2021-110-003	Unable to turn	No	Normal	Damage	No	Inner diameter runout 4
	2021-110-002	Rotatable	No	Normal	Damage	No	Inner diameter runout 3

According to the fault records of the motorized spindle, the type and number of faults are sorted out. The results of the classification of the fault data for the motorized spindle are listed in Tabel 2.

Table 2. Failure data rectification table.

Failure type	Number of failures	Failure frequency
Shaft failure	58	0.1191
Strike	1	0.0021
Motor failure	42	0.0862
Bearing failure	205	0.4209
Plug a leak or blockage	8	0.0164
Accuracy failure	173	0.3552

Among the fault types of motorized spindles, bearing damage accounts for a large proportion, approximately 42%, the accuracy accounts for the second, approximately 35%, and the

damage proportion of rotating shaft and motor is similar, which is approximately 10%. The remaining fault factors are less affected, all below 2%.

B. Fault tree modeling of motorized spindle system

The motorized spindle system of the cycloid gear grinding machine was divided according to the tree-building rules, and fault events at all levels were defined. The fault in a motorized spindle is defined as a top event (T). The main phenotypic form of motorized spindle failure is defined as an intermediate event (M).

The most direct factor causing failure was defined as the bottom event (X), and the results are listed in Table 3. The fault tree of the motorized spindle system is shown in Figure.2.

Table 3. Event code of motorized spindle failure

Code	Event	Code	Event	Code	Event
M1	The motorized spindle heats up	X1	The built-in motor overheats	X13	The air gap is too small
M2	The spindle rotates abnormally	X2	Bearing damage	X14	Poor lubrication
M3	High vibration and noise	X3	Insufficient bearing lubrication	X15	The air gap between the stator and rotor is uneven
M4	Difficulty starting	X4	Improper bearing preload	X16	Poor spindle dynamic balance
M5	Other	X5	The cooling water path is not smooth	X17	The motor parameters are set incorrectly
Code	Event	Code	Event	Code	Event

M6	Bearing failure	X6	The water jacket is leaking	X18	The stator lead wire is connected incorrectly
M7	Cooling system failure	X7	Improper assembly	X19	The stator and rotor air gap is too small
M8	The spindle speed error is too large	X8	Sensor failure	X20	The stator windings are damaged
M9	Spindle speeder	X9	Servo cable failure	X21	The power supply is out of phase
M10	The spindle speed is unstable	X10	The rotor is out of magnetism	X22	The seal is not tight
M11	Sweep	X11	The supply voltage is unstable		
M12	Motor failure	X12	Impurities invade, bearing wear		

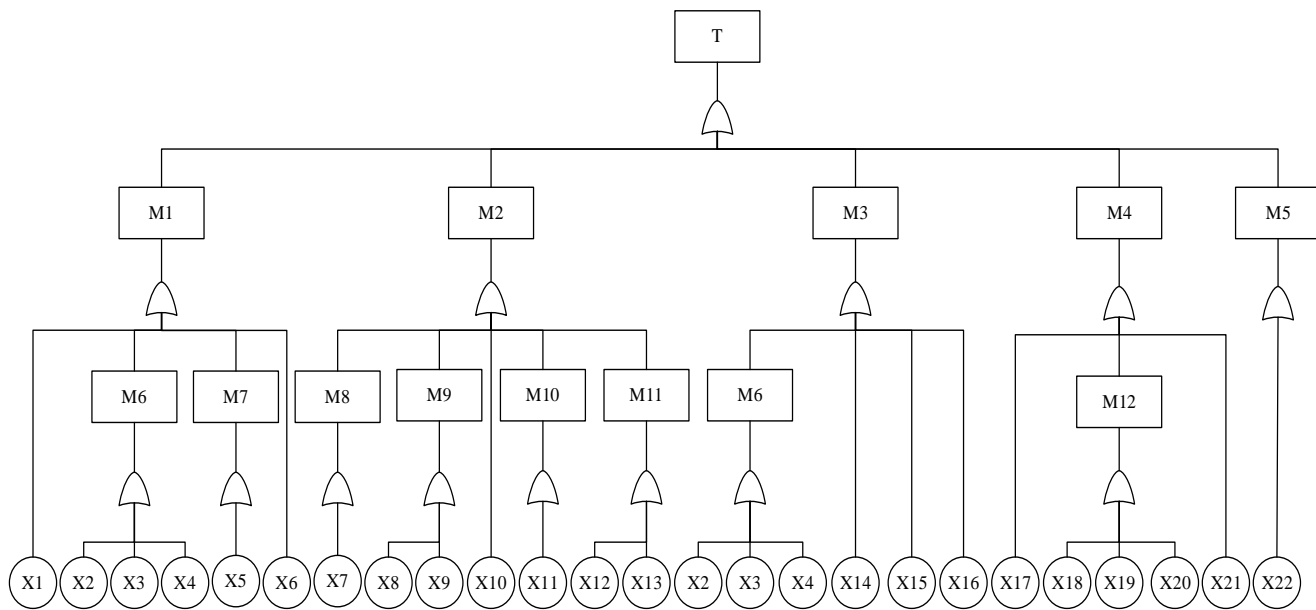


Fig. 2. Fault tree of motorized spindle of cycloid gear grinding machine.

C. spindle fuzzy quantitative analysis

1) Bottom event fuzzy probability

The fault tree structure of a motorized spindle is complex, and the number of bottom events is large. However, obtaining relevant statistical data on certain events is difficult. Therefore, this section uses the expert investigation method to perform a fuzzy evaluation and converts the fuzzy language into a fuzzy probability to evaluate the fault tree of the motorized spindle.

The fuzzy probability of each bottom event is obtained using an expert scoring method. Owing to the uncertainty in the occurrence of fault events, different experts have different degrees of fuzzy descriptions of the probability of an event. Generally, the fuzzy evaluation language can be divided into five levels. The fuzzy interval number corresponding to each evaluation language value and its membership function are listed in table 4, and the order of magnitude of the membership function is 10^{-4} .

Table 4. Language variable transformation rules.

Term	Language variables	Membership function (a,m,b) .
Very small	VS	$(0,0,0.3)$
Small	S	$(0.1,0.3,0.5)$
Medium	M	$(0.3,0.5,0.7)$
High	L	$(0.5,0.7,0.9)$
Very high	VL	$(0.7,1.0,1.0)$

The evaluation coefficient and proportion of evaluations were calculated according to the industry education level and working hours of the survey experts. The results are listed in table 5.

Table 5. Rating Weight Table.

Grade R	Number of experts MR	Evaluation coefficient VR	Evaluation weight w_r
1	2	0.8	0.1084
2	4	0.7	0.0964
3	3	0.6	0.0843
4	2	0.5	0.0723

The fuzzy probability value of an event can be obtained by using a fuzzy evaluation language. The process is as follows:

$$P_{xj} = \sum_{i=1}^l w_{VS_i} \times (a, m, b)_{VS} + \sum_{i=1}^k w_{S_i} \times (a, m, b)_S + \sum_{i=1}^t w_{M_i} \times (a, m, b)_M + \sum_{i=1}^q w_{L_i} \times (a, m, b)_L + \sum_{i=1}^p w_{VL_i} \times (a, m, b)_{VL} \quad (1)$$

Where $l + k + t + q + p = 11$ and l, k, t, q and p are used to evaluate the number of experts whose language is VS, S, M, L

and $VL, w_{VS_i}, w_{S_i}, w_{M_i}, w_{L_i}$ and w_{VL_i} representing the weight of each expert whose evaluation value is VS, S, M, L and VL .

Considering event X5 as an example, the evaluation languages were $S, M, S, M, VS, VS, S, S, H, S$, and VS . The fuzzy probability can be calculated using Formula (1) as (1.58E-05,3.05E-05,5.31E-05). The fuzzy probabilities of all bottom events were calculated and summarized. The results are listed in Table 6.

Table 6. Bottom event fuzzy probability table.

The bottom event code	Fuzzy probability values	The bottom event code	Fuzzy probability values
X1	(2.28E-05,4.28E-05,6.28E-05)	X12	(3.05E-05,5.05E-05,7.05E-05)
X2	(4.73E-05,6.93E-05,8.54E-05)	X13	(1.37E-05,3.01E-05,5.19E-05)
X3	(3.92E-05,5.91E-05,7.91E-05)	X14	(1.72E-05,3.34E-05,5.53E-05)
X4	(4.06E-05,6.06E-05,8.06E-05)	X15	(6.39E-06,1.92E-05,4.28E-05)
X5	(1.58E-05,3.05E-05,5.31E-05)	X16	(1.81E-05,3.06E-05,5.43E-05)
X6	(1.12E-05,2.40E-05,4.76E-05)	X17	(2.82E-05,4.52E-05,6.51E-05)
X7	(1.75E-05,2.98E-05,5.36E-05)	X18	(2.34E-05,3.70E-05,5.85E-05)
X8	(1.20E-05,2.89E-05,5.05E-05)	X19	(2.06E-05,3.43E-05,5.75E-05)
X9	(2.70E-05,4.34E-05,6.52E-05)	X20	(3.40E-05,5.33E-05,7.22E-05)
X10	(1.33E-05,2.24E-05,4.78E-05)	X21	(3.52E-05,5.63E-05,7.16E-05)
X11	(2.46E-05,4.19E-05,6.18E-05)	X22	(1.57E-05,3.20E-05,5.39E-05)

2) Top event fuzzy probability calculation

The fuzzy OR gate output formula of fault tree structure function is as follows:

$$\tilde{P}_{OR} = [1 - \prod_{i=1}^n (1 - a_i), 1 - \prod_{i=1}^n (1 - m_i), 1 - \prod_{i=1}^n (1 - b_i)] \quad (2)$$

Where \tilde{P}_{OR} is the output of the fuzzy OR gate, n is the number of bottom events contained in intermediate event. a_i, m_i

and b_i correspond to the membership function of the i -th event respectively

Combined with Formula (2), the fuzzy probability table of the intermediate and top events can be calculated. The results are listed in Table 7.

Table 7. Intermediate event fuzzy probability table.

Event code	Fuzzy probability values	Event code	Fuzzy probability values
M1	(1.77E-04,2.86E-04,4.09E-04)	M7	(1.58E-05,3.05E-05,5.31E-05)
M2	(1.39E-04,2.47E-04,4.01E-04)	M8	(1.75E-05,2.98E-05,5.36E-05)
M3	(1.69E-04,2.72E-04,3.97E-04)	M9	(3.90E-05,7.23E-05,1.16E-04)
M4	(1.41E-04,2.26E-04,3.25E-04)	M10	(2.46E-05,4.19E-05,6.18E-05)
M5	(1.57E-05,3.20E-05,5.39E-05)	M11	(4.42E-05,8.06E-05,1.22E-04)
M6	(1.27E-04,1.89E-04,2.45E-04)	M12	(7.79E-05,1.25E-04,1.88E-04)

The fuzzy probability of the top-event motorized spindle fault can then be obtained using Formula (2).

$$P_T = (0.64E - 03, 1.06E - 03, 1.58E - 03) \quad (3)$$

As shown in Formula (3), the minimum probability of failure of the motorized spindle is $0.64E - 03$, the maximum is $1.58E - 03$, and the possibility of its value being $1.06E - 03$ is

the highest.

The form of λ cut set for P_T is as follows:

$$P_{T\lambda} = \left(\left((1.06E-03) - (4.22E-04) \right) + (4.22E-04)\lambda \right) \left(\left((1.06E-03) + (5.22E-04) \right) - (5.22E-04)\lambda \right) \quad (4)$$

When $\lambda=0$, the fault probability of motorized spindle is

fuzzy interval: $P_{T\lambda} = (6.41E-04, 1.58E-03)$; when $\lambda=0$, $P_{T\lambda}$ is a fixed value: $P_{T\lambda}=1.06E-03$. When the value interval is 0.1, the fuzzy probability of the top event changing with the confidence level is obtained, as listed in table 8.

Table 8. Fuzzy probability of top event changing with confidence level.

Confidence level λ	$\alpha=\beta$	Confidence level λ	$\alpha=\beta$
0.1	(6.83E-04,1.53E-03)	0.6	(8.94E-04,1.27E-03)
0.2	(7.25E-04,1.48E-03)	0.7	(9.36E-04,1.22E-03)
0.3	(7.68E-04,1.43E-03)	0.8	(9.78E-04,1.17E-03)
0.4	(8.10E-04,1.38E-03)	0.9	(1.02E-03,1.12E-03)
0.5	(8.52E-04,1.32E-03)	1.0	(1.06E-03,1.06E-03)

3) Bottom event fuzzy importance calculation

The fuzzy probability of the top event is (0.64E-03,1.06E-03,1.58E-03), where mid-value $m_{T_e}=1.09E-3$. Assuming that the occurrence probability of X1 is 0, the fuzzy probability of the top event can be calculated as: (0.61E-03,1.02E-03,1.52E-03),

where the mid-value is $m_{T_e}=1.05E-3$. Subsequently, the fuzzy importance of bottom event X1 is. Similarly, by calculating the other 21 bottom events, the fuzzy importance of each event can be obtained, as listed in Table 9, and drawn as a vertical diagram, as shown in Figure 3.

Table 9. Bottom event fuzzy importance table.

The bottom event code	Fuzzy importance	The bottom event code	Fuzzy importance	The bottom event code	Fuzzy importance
X1	4.27E-05	X9	4.47E-05	X17	4.58E-05
X2	1.36E-04	X10	2.64E-05	X18	3.89E-05
X3	1.18E-04	X11	4.25E-05	X19	3.66E-05
X4	1.21E-04	X12	5.04E-05	X20	5.31E-05
X5	3.24E-05	X13	3.14E-05	X21	5.48E-05
X6	2.66E-05	X14	3.48E-05	X22	3.34E-05
X7	3.26E-05	X15	2.18E-05		
X8	3.01E-05	X16	3.34E-05		

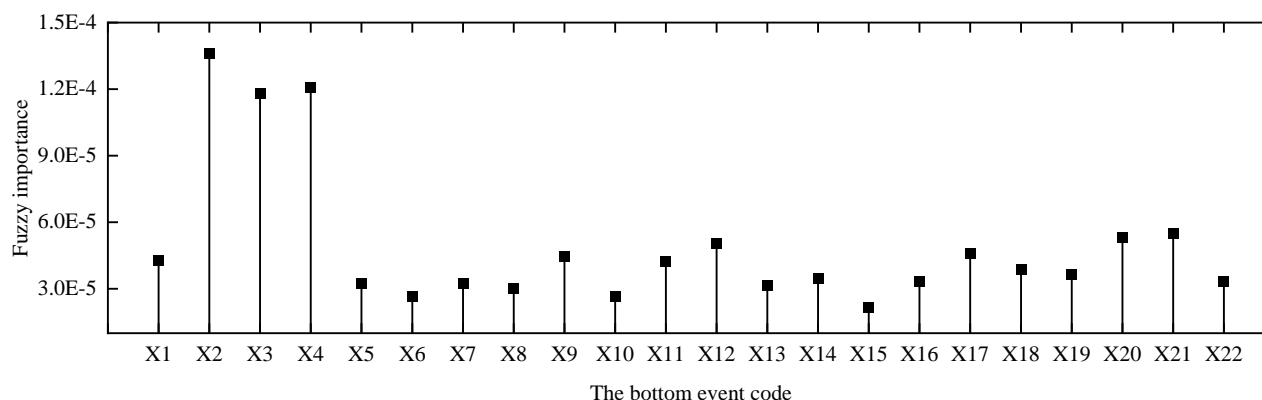


Fig. 3. Fuzzy probability vertical diagram of motorized spindle bottom event.

The fuzzy importance of each bottom event is sorted as follows: $X_2 > X_4 > X_3 > X_{21} > X_{20} > X_{12} > X_{17} > X_9 > X_1 > X_{11} > X_{18} > X_{19} > X_{14} > X_{22} > X_{16} > X_7 > X_5 > X_{13} > X_8 > X_6 > X_{10} > X_{15}$. From the results, the main factors causing the failure of the motorized spindle were X_2 bearing scuffing, improper preload of the X_4 bearing, insufficient lubrication of the X_3 bearing, lax sealing of X_{21} , and damage to the X_{20} stator winding. Among them, X_2 , X_4 , and X_3 are bearing damages that must be considered in the process of production and use. Improving or solving such faults will improve the reliability of motorized spindles more effectively.

3. Reliability simulation of motorized spindle

With the development of CNC machine tool technology, its internal structure has become more complex, and the factors leading to failure have become increasingly complex. This increases the difficulty in determining the reliability and performance of the entire equipment through physical tests and mathematical models. To solve this problem, it is becoming increasingly important to study reliability simulation technologies.

In this section, the fault tree model is used to optimize the Monte Carlo simulation. The fault tree of the motorized spindle was used as the logic of the reliability simulation to complete the reliability simulation of the motorized spindle and verify its effectiveness and rationality.

A. Fuzzy Fault Tree-Monte Carlo Introduction

This section introduces the tree-Monte Carlo reliability simulation. The fault-tree model of the motorized spindle described in Section 3 was used as the logical relationship in the reliability simulation. The analysis process is as follows:

1) Establish simulation model

In the simulation model, T was used to represent the system state of the motorized spindle, where there were n bottom events. The state of each bottom event can be represented by x_i ($i = 1, 2, \dots, n$), and the failure probability function can be represented by $F_i(t)$. It is assumed that these bottom events are independent of each other, and each bottom event has only two states of 'happening' and 'not happening', represented by x_i . The rules are as follows:

$$x_i(t) = \begin{cases} 0, & \text{Indicates that the } i \text{ th bottom event did not occur at } t \\ 1, & \text{denotes that the } i \text{ th bottom event has occurred at } t \end{cases} \quad (5)$$

There are only two working states of the motorized spindle, namely failure and no failure, which are expressed by $T(t)$. The rules are as follows:

$$T(t) = \begin{cases} 0, & \text{Electric spindle failure at time } t \\ 1, & \text{The motorized spindle is normal at time } t \end{cases} \quad (6)$$

The structural function of the fault tree of the motorized spindle system can be expressed as $T[X(t)]$

$$\begin{cases} T(t) = T[X(t)] \\ X(t) = [x_1, x_2, \dots, x_i, \dots, x_n] \end{cases} \quad (7)$$

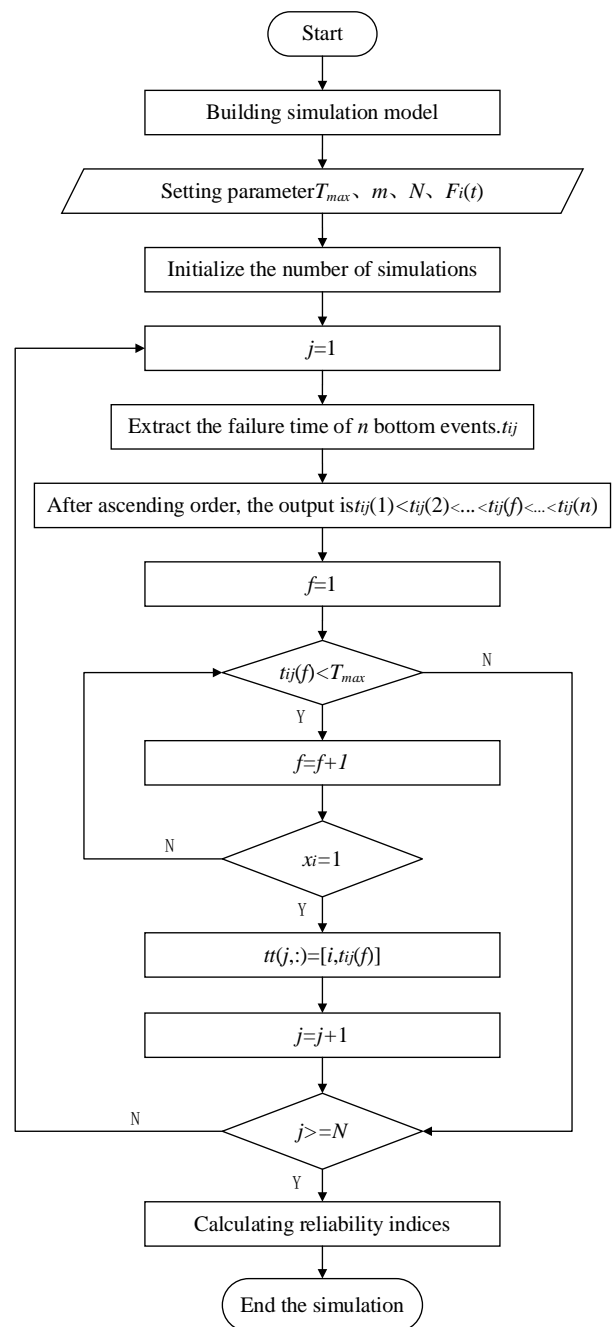


Fig. 4. Fault tree-Monte Carlo simulation flow chart.

2) Simulation parameter setting

First, the maximum working time of the motorized spindle is set to T_{max} . Note that the simulation life of most motorized spindles should be less than T_{max} , which is to ensure that the simulation results are relatively complete.

Then $(0, T_{max})$ is divided into m stages, namely: $[0, t_1], [t_1, t_2], \dots, [t_{r-1}, t_r], \dots, [t_{m-1}, t_m]$, then each stage is represented as follows:

$$\Delta t = \frac{T_{max}}{m} \quad (8)$$

The number of simulations was set to N . In general, the larger the number of simulations, the more accurate the simulation results; however, the larger the number of simulations, the longer the calculation time. Therefore, it needs to be determined after multiple calculations.

3) Bottom event failure sampling

First, the cumulative failure distribution function $F_i(t)$ is obtained for each bottom event. The time-sampling t_i of the failure of the i -th bottom event is as follows:

$$t_i = F_i^{-1}(\eta) \quad (9)$$

where $F_i^{-1}(\eta)$ is the inverse function of $F_i(t)$, and η is a random number in $[0, 1]$.

In the j -th run, the time sampling for the failure of the i -th bottom event is as follows:

$$t_{ij} = F_i^{-1}(\eta_{ij}) \quad (10)$$

where η_{ij} is a random number for the i -th bottom event during the j -th run.

The working state of the i -th bottom event at time t is represented by $x_i(t)$ as follows:

$$x_i(t) = \begin{cases} 0, & t < t_{ij} \\ 1, & t \geq t_{ij} \end{cases} \quad (11)$$

After j runs, a set of time-sampling data for the failure of each bottom event is generated: $t_{1j}, t_{2j}, \dots, t_{ij}, \dots, t_{nj}$, and the data are sorted in ascending order: $t_{ij}(1) < t_{ij}(2) < \dots < t_{ij}(f) < \dots < t_{ij}(n)$.

4) Test the structure function

According to the sorted events, the failure of the motorized spindle x_f was judged, and the bottom event that caused the failure was identified. The failure time $t_{ij}(f)$ and the corresponding bottom event number i are included in T . After N runs, a set of matrices $N \times 2 [i, t_{i1}(f); i, t_{i2}(f); \dots; i, t_{ij}(f); \dots; i, t_{iN}(f)]$ is obtained, which is the failure time of the motorized spindle in this simulation. The first column number in the matrix was counted, and the number of times each bottom event caused the

failure of the motorized spindle was obtained.

5) Reliability index calculation method

(1) MTBF

The system failure time obtained in N simulations is retained in the matrix, and the Mean Time Between Failure (MTBF) of the motorized spindle can be obtained as follows:

$$\text{MTBF} = (\sum_{j=1}^N t_{ij}(f))/N \quad (12)$$

(2) Unreliability and reliability

For the failure number Δm_r of the motorized spindle in each interval $[t_{r-1}, t_r]$ ($r = 1, 2, \dots, m$), the failure number of the motorized spindle in $[0, t_r]$ is $m_r = \sum_{i=1}^r \Delta m_i$. When the running time reaches t_r , the point estimation value $\hat{F}(t)$ of the failure probability of the motorized spindle can be expressed as follows:

$$\hat{F}(t_r) = \sum_{i=1}^r \Delta m_i / N \quad (13)$$

The reliability point estimate $\hat{R}(t)$ can be expressed as follows:

$$\hat{R}(t_r) = 1 - \hat{F}(t_r) \quad (14)$$

(3) Failure probability density $f(t)$

$f(t)$ represents the probability of top event failure at a certain time, and represents the trend of system failure probability changing with time. The point estimate can be expressed as follows:

$$\hat{f}(t_r) = \Delta m(r)/N \quad (15)$$

(4) The importance of each bottom event

In the Monte Carlo simulation, the frequency of the i -th bottom event that causes the failure of the motorized spindle is considered important in the entire system; that is,

$$W(x_i) = \frac{\text{Number of system failures caused by event } i}{\text{Total number of system failures}} \quad (16)$$

B. Fault tree-Monte Carlo simulation results analysis

1) Mean time between failures

The maximum running time was set to 10,000 h, and the time interval was 10,000. The average fault-free time of the motorized spindle was obtained through 100 times, 1000 times, 5000 times, 10,000 times, 50,000 times, and 100,000 times of simulations, as listed in Table 10.

With an increase in the number of simulations, the average fault-free time of the motorized spindle gradually stabilized. Considering the calculation time and accuracy of the results, the results of 50,000 simulations were selected for the analysis, and the estimated value of the motorized spindle MTBF was

approximately 2817.7 h.

Table 10. Multi-source Bayes-Monte Carlo simulation results.

NS	MTBF
100	3073.0775
1000	2803.6337
5000	2835.5511
10000	2851.4475
50000	2817.6716

2) Failure probability density curve

The change in the system failure rate over time is described, which can provide ideas for the prediction and analysis of failure probability. The failure probability density curves for different periods are shown in Figure.5. It can be observed that as the number of simulations increases, the trend of the curve gradually stabilizes.

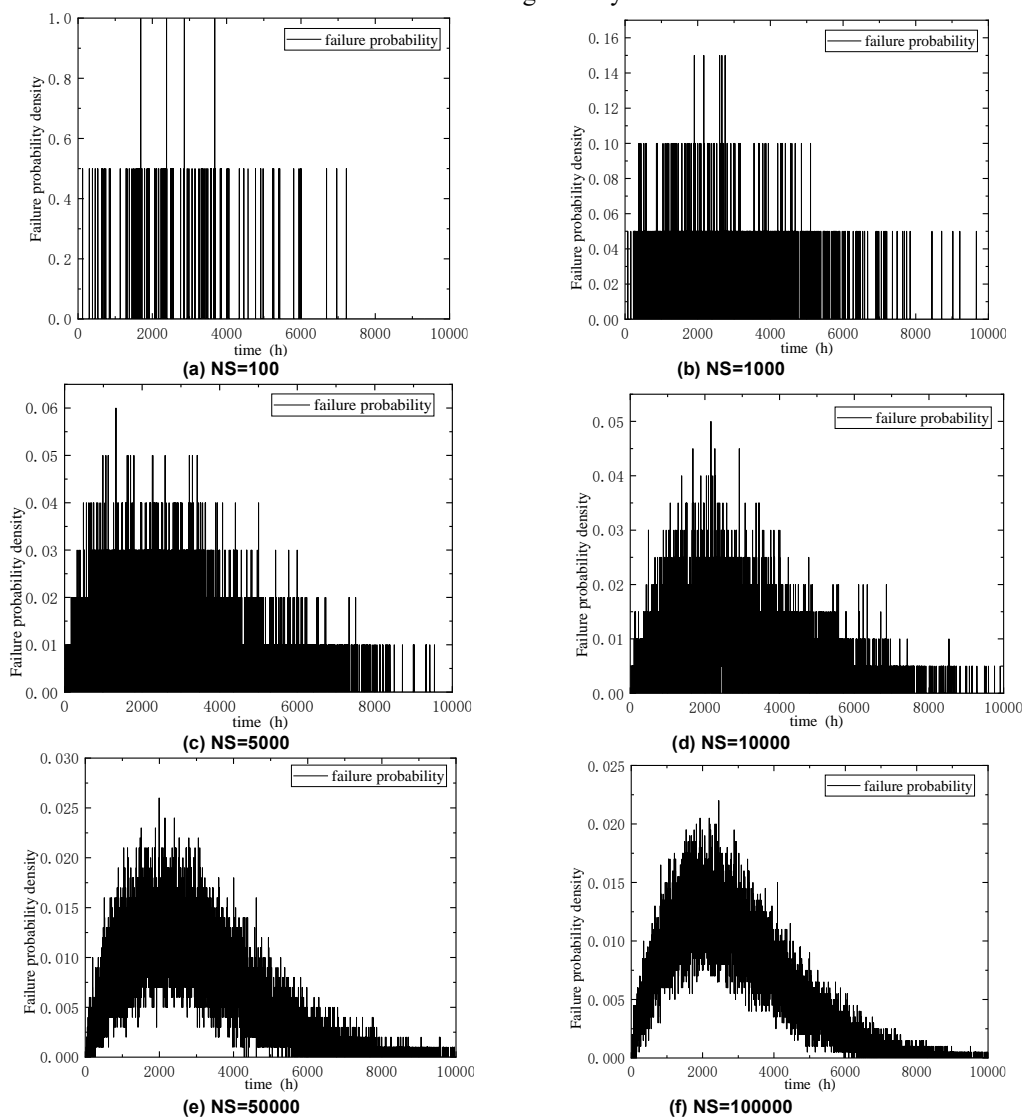


Fig. 5. Fault probability density curve of motorized spindle.

C. Analysis of bottom event

The simulation importance of the 22 bottom events was calculated using formula. The results are listed in table 11; the fuzzy importance must be converted into a percentage when performing an error comparison. As shown in Figure 6, the results of the simulation importance were approximately the same as those of fuzzy fault tree quantitative analysis, and the more important factors were X2, X4, X3, X21, and X20. Among

them, X2, X4, and X3 are the bearing damages, and their importance in the simulation was higher than that in the evaluation. Therefore, attention should be paid to the production and use processes. Improving these problems will improve the reliability of motorized spindles. The error between the results and the fuzzy importance was small, and the order of importance of the bottom event was almost consistent with the theoretical calculation results, which verified the accuracy of

the Monte Carlo simulation program in predicting the importance of the bottom event.

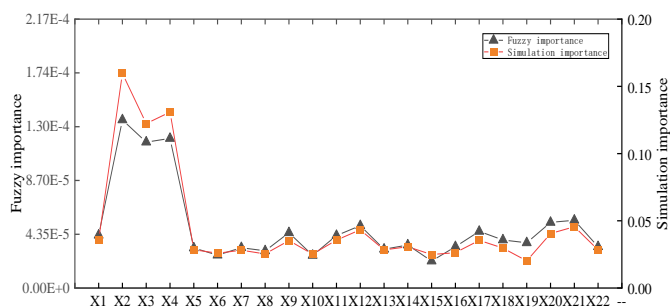


Fig. 6. Comparison of bottom event importance.

Table 11. Importance comparison table of bottom event simulation.

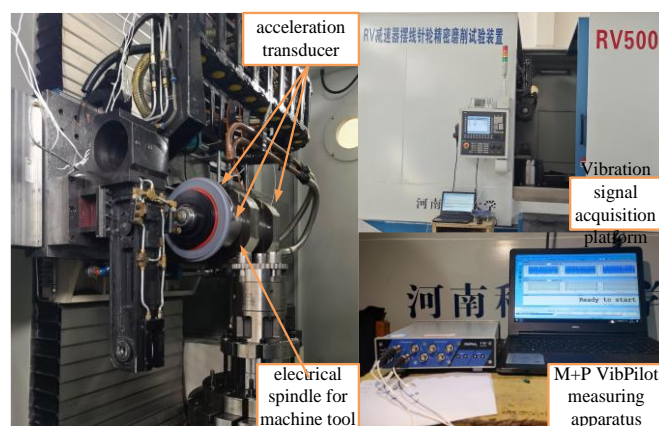
Bottom event number	Fuzzy importance	Simulation importance	Error
X1	4.27E-05	0.0358	0.35%
X2	1.36E-04	0.1596	-3.45%
X3	1.18E-04	0.1223	-1.38%
X4	1.21E-04	0.1308	-1.95%
X5	3.24E-05	0.0285	0.13%
X6	2.66E-05	0.0259	-0.14%
X7	3.26E-05	0.0281	0.19%
X8	3.01E-05	0.0254	0.23%
X9	4.47E-05	0.0353	0.58%
X10	2.64E-05	0.0252	-0.09%
X11	4.25E-05	0.0357	0.34%
X12	5.04E-05	0.0433	0.30%
X13	3.14E-05	0.0284	0.05%
X14	3.48E-05	0.0307	0.13%
X15	2.18E-05	0.0249	-0.49%
X16	3.34E-05	0.0263	0.44%
X17	4.58E-05	0.0355	0.66%
X18	3.89E-05	0.0297	0.61%
X19	3.66E-05	0.0202	1.35%
X20	5.31E-05	0.0405	0.83%
X21	5.48E-05	0.0456	0.48%
X22	3.34E-05	0.0284	0.23%

4. Vibration experiment of motorized spindle

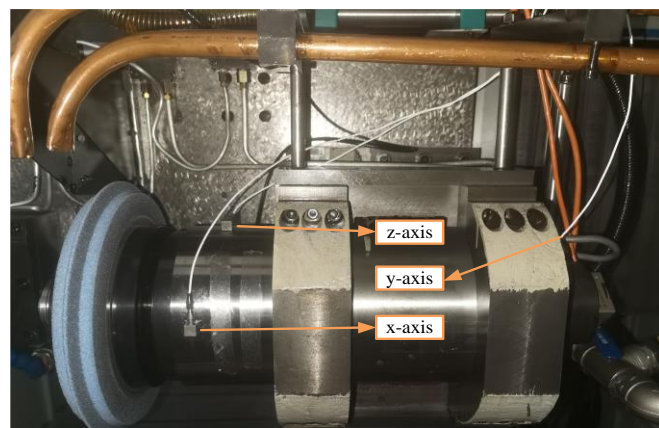
A motorized spindle is a core component of a cycloid gear grinding machine, and its performance and reliability directly affect the machining quality of the machine tool [30]. The

reliability of a motorized spindle in long-term processing gradually declines, its remaining life gradually decreases, and the possibility of failure gradually increases. Failure of a motorized spindle directly affects the quality of the product and causes serious economic losses. Therefore, it is important to determine the problem of motorized spindle failure promptly and select an appropriate maintenance method [31] to reduce the impact of motorized spindle failure on normal production. This section considers a motorized spindle bearing as the research object to study the fault feature extraction method based on wavelet packets and empirical mode decomposition.

The motorized spindle produces many vibration signals containing characteristic information during the working process, which must be collected before fault analysis and diagnosis. Rolling bearings are commonly used in motorized spindles [32]. The vibration-signal test platform is shown in Figure.7(a). It mainly includes a cycloid gear grinding machine spindle, an M+P VibPilot measuring instrument, and an acceleration sensor.



(a) Vibration signal acquisition device of motorized spindle



(b) Sensor arrangement

Fig. 7. The vibration signal test platform.

1) Introduction of experimental equipment

(1) By querying the instruction manual of the cycloid gear grinding machine, it is known that the motorized spindle model is HGE-MD230Z3.

(2) The experimental equipment M+P VibPilot can support up to 204.8 kHz, 24-bit synchronous sampling, and eight analog input channels. The acceleration sensor sensitivity range is 90-105 mv / g, the sampling frequency is 2048 Hz, and the sampling time is 5 s.

2) Experimental steps

The experimental equipment was connected, and an appropriate position on the motorized spindle was selected to fix the acceleration sensor. The sensor measuring points are arranged in the axial and radial directions of the motorized spindle, as shown in Fig.7(b), and the relevant parameters are set in the software to check whether each channel is working properly. The speed of the motorized spindle is adjusted and, vibration signals are collected after its stable operation. The motorized spindle speed is adjusted to 1000 rpm, 1400 rpm, 1800 rpm, 2200 rpm, 2600 rpm, and 3000 rpm, and step (3) is

repeated.

3) Vibration signal denoising

Considering 2600 rpm as an example, the time-domain diagram is shown in Figure.8.

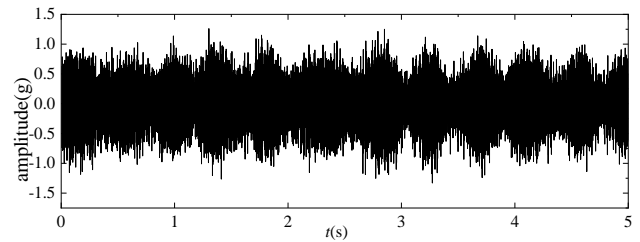


Fig.8. Time domain diagram of vibration signal at 2600 rpm.

The horizontal and vertical axes represent the sampling time and vibration acceleration, respectively. Three wavelet packet decomposition layers were selected, and the obtained signal decomposition diagram is shown in Figure 9. As can be seen from Figure 9, the wavelet packet decomposition results corresponding to the G-graph have higher energy than other results. The signal of the energy distribution of all the nodes in the last layer was calculated, and the value is shown in Figure 10.

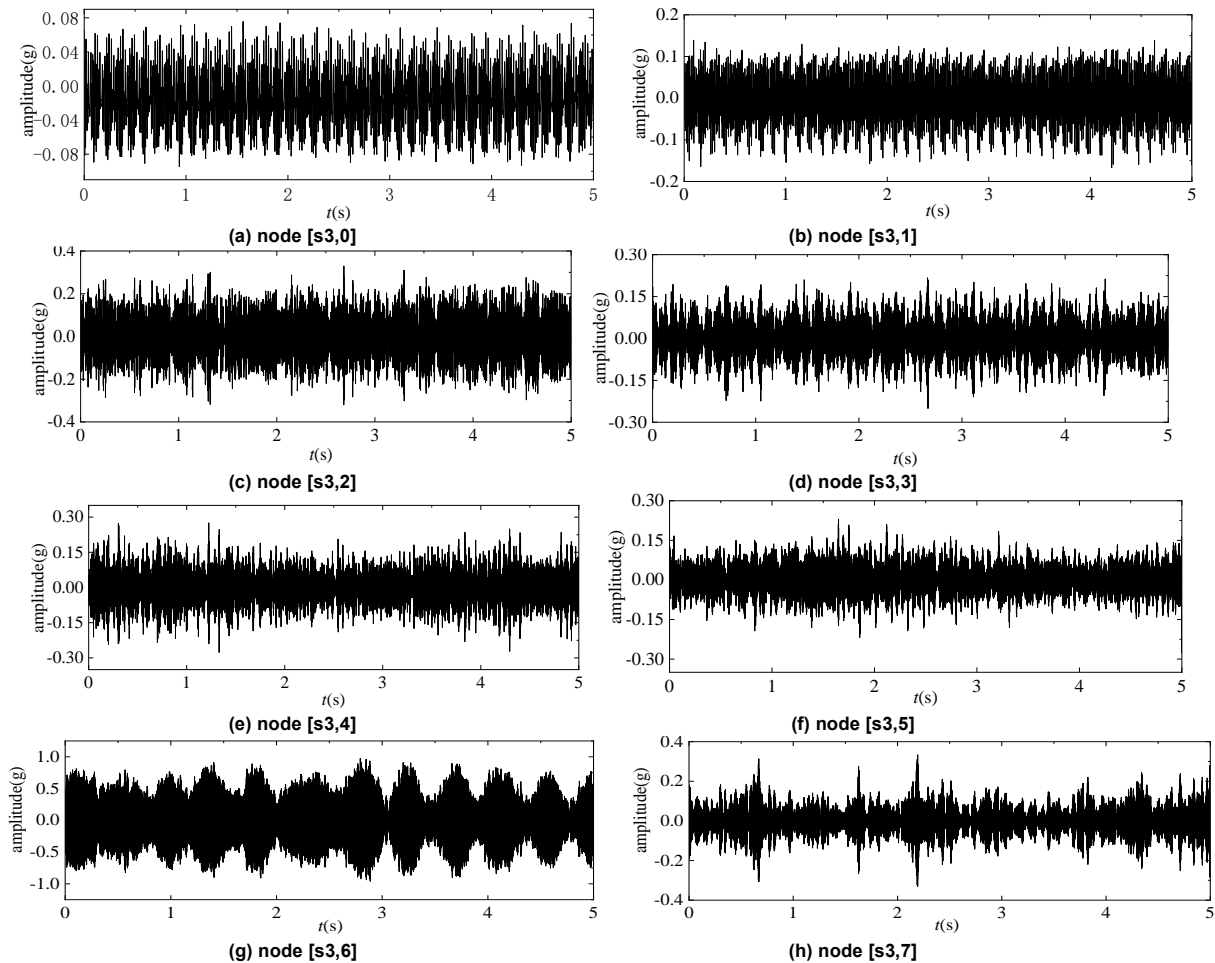


Fig. 9. Signal reconstruction by wavelet packet decomposition.

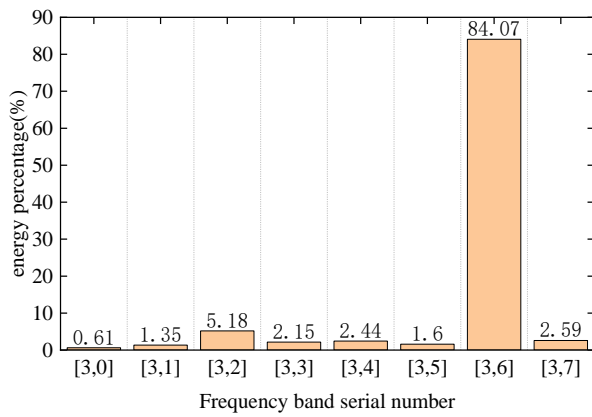


Fig. 10. Fault data type.

Figure 10 shows that the signal energy corresponding to the node [3,6] accounts for 84.07%, and the remaining signal energy accounts for less than 10%. It can be observed that the frequency of the original signal is distributed in this node, and the other nodes are the frequency distribution of the noise signal. Therefore, the node signal is regarded as a component of wavelet packet reconstruction.

This method was used to process vibration signals at different speeds, and the results are shown in Figure 11. It can be seen from Figure 11 that the strength of vibration has a certain correlation with the speed of rotation.

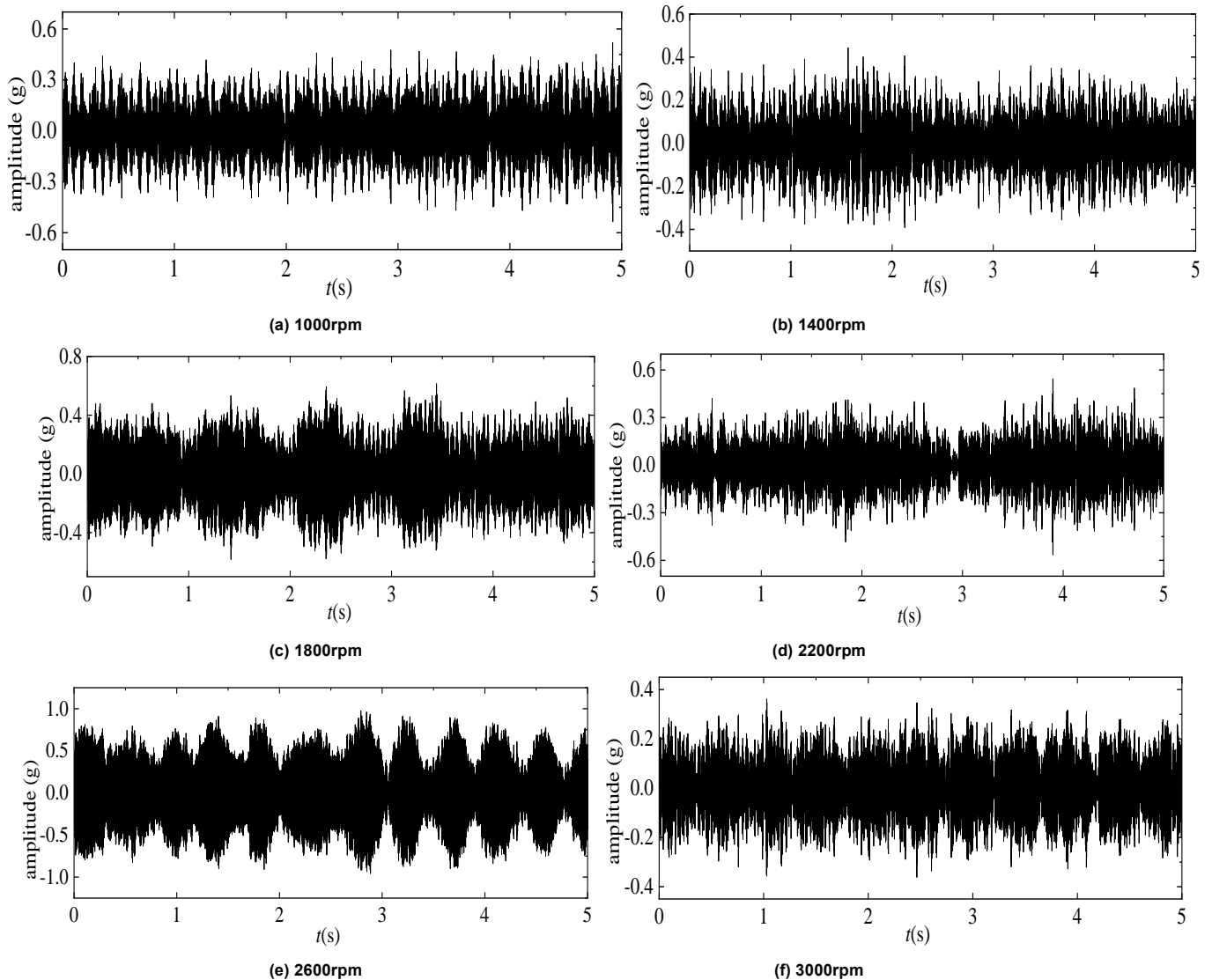


Fig. 11. Wavelet packet decomposition and reconstruction signals at different speeds.

4) Empirical mode vibration signal decomposition

Considering the vibration signal at 2600 rpm as an example, the signal denoised by the wavelet packet was decomposed using EMD, and the fault characteristics of the signal were extracted. After completing the EMD iteration, eight IMF

components and one residual component were obtained. Here, the first five IMF components were used for spectrum processing to obtain the IMF time-frequency diagram, as shown in Figure 12.

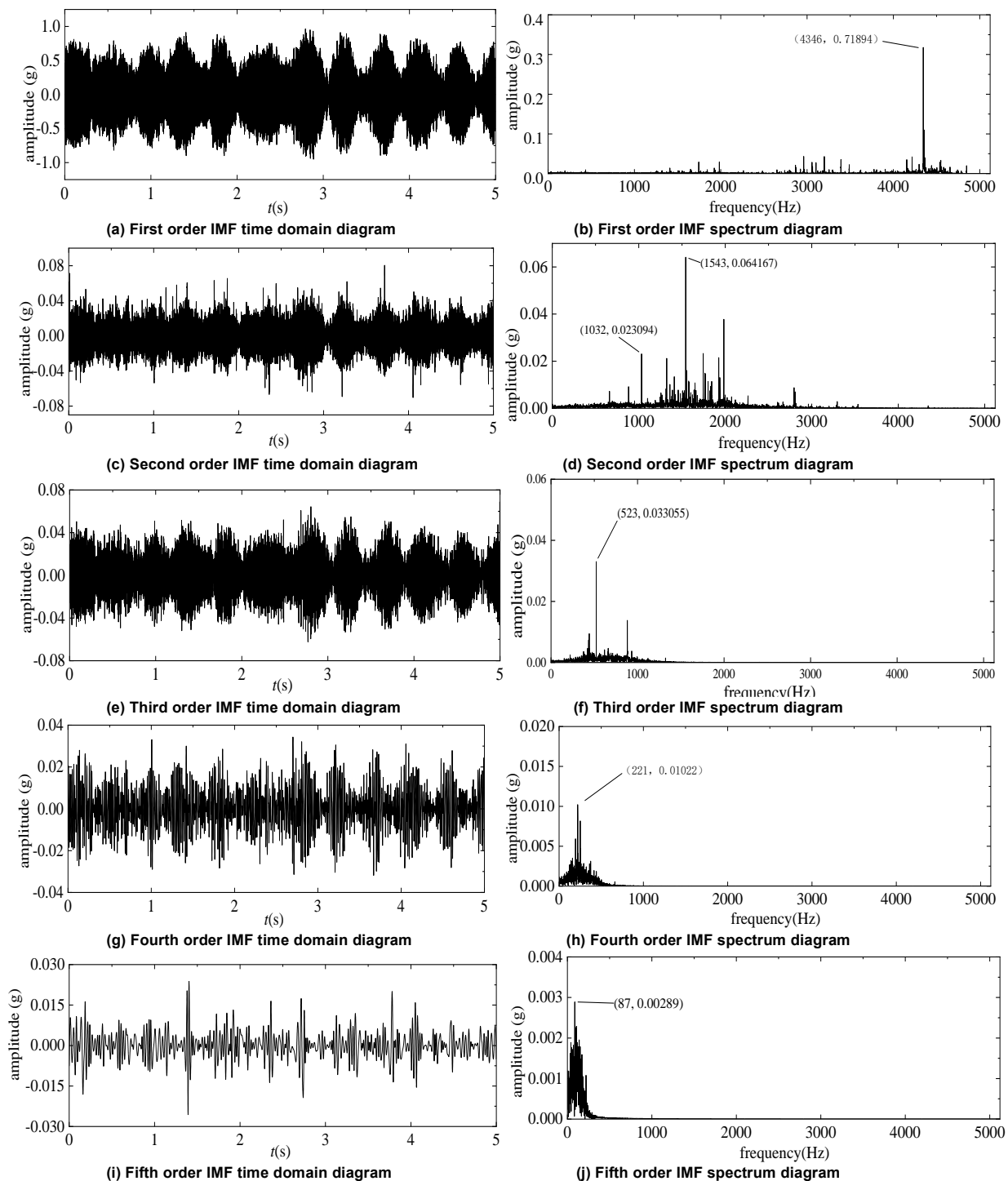


Fig. 12. The first to fifth IMF components of EMD decomposition.

The peak characteristic components of the different frequency bands in the vibration signal are reflected in the first fifth-order IMF components. From the IMF spectrum diagram shown in Figure 12, it can be observed that there are peaks at the points of the double shaft frequency in the fifth-order IMF, 523 Hz in the third-order IMF, and 1032 Hz and 1543 Hz in the second-order IMF. By comparing the peak information with the fault characteristic frequency of the motorized spindle structure, it was observed that the peak information was highly correlated

with the frequency-doubling relationship of the fault characteristic frequency 514.97 Hz of the motorized spindle, and the bearing fault could be diagnosed accordingly.

Therefore, the fault diagnosis method based on wavelet packets and empirical mode decomposition can be used to detect the state of the motorized spindle bearing, identify the bearing fault in advance, arrange the motorized spindle to return to the factory for timely maintenance, prolong the effective life of the motorized spindle, and improve its reliability level.

5. CONCLUSION

Based on field investigations and relevant literature, a fuzzy fault tree analysis of the motorized spindle of a cycloid gear grinding machine was conducted. After the calculation, the fuzzy failure probability of the motorized spindle top event and the three faults with higher fuzzy importance were all bearing faults. An FTA-Monte Carlo simulation model of a motorized spindle was established. Considering the bearing fault as an example, the comprehensive posterior distribution is calculated using the multi-source Bayes method and is taken as the parameter distribution of the bearing in the reliability simulation.

The reliability simulation was performed several times, and the simulation results of 50,000 times were selected. The

estimated value of the MTBF of the motorized spindle was approximately 2817.7 h, and the reliability, unreliability curves, and probability density curves were drawn. Comparing the results with those in the third chapter, it was observed that the error was small, and the feasibility and accuracy were verified. Finally, a vibration test of the motorized spindle bearing was conducted. Considering 2600 rpm as an example, the collected initial signal was denoised using the wavelet packet transform, and nodes with higher energy were selected as the denoised signals. Subsequently, the EMD method is used to decompose and reconstruct it, and the fault characteristics of the motorized spindle bearing in the signal are analyzed to complete the fault feature extraction.

Acknowledgement

This work was supported in part by the Provincial Science and Technology Research and Development Program Joint Fund under Grant 222103810040, in part by the 2023 Key scientific research of universities in Henan Province Project, under Grant 23A460017

References

1. Nilesh P, Bhatt M G, Multicriteria FMECA based decision-making for aluminum wire process rolling mill through COPRAS-G. *Journal of Quality and Reliability Engineering* 2016; 9, <https://doi.org/10.1155/2016/8421916>.
2. Gajanand G, Rajesh P M, Comparative analysis of traditional and fuzzy FMECA approach for criticality analysis of conventional lathe machine. *International Journal of System Assurance Engineering and Management* 2020; 11(2): 379-386, <https://doi.org/10.1007/s13198-019-00938-y>
3. Lee G H, Akpudo U E, Hur J W, FMECA and MFCC-based early wear detection in gear pumps in cost-aware monitoring systems. *Electronics* 2021; 10(23), <https://doi.org/10.3390/electronics10232939>
4. Fabiś – Domagała J, Momeni H, Domagała M, Matrix FMEA analysis as a preventive method for quality design of hydraulic components. *System Safety: Human - Technical Facility - Environment* 2019; 1(1): 684-691, <https://doi.org/10.2478/czoto-2019-0087>
5. Soltanali H, Khojastehpour M, Farinha J T, An integrated fuzzy fault tree model with Bayesian network-based maintenance optimization of complex equipment in automotive manufacturing. *Energies* 2021; 14(22): 7758, <https://doi.org/10.3390/en14227758>
6. Qian C, Li W J, Ren Y, Monte-Carlo simulation-based analysis for structural reliability of the crane rail beam under stochastic crane movements and irradiation conditions. *Quality and Reliability Engineering International* 2023; 39(5): 1704-1719, <https://doi.org/10.1002/qre.3293>
7. Wang S X, Yao Y T, Ge D C, Reliability evaluation of standby redundant systems based on the survival signatures methods. *Reliability Engineering & System Safety* 2023; 239: 109509, <https://doi.org/10.1016/j.ress.2023.109509>
8. Zhu D P, Ding Z X, Probabilistic modeling for long-term fatigue reliability of wind turbines based on Markov model and subset simulation. *International Journal of Fatigue* 2023; 173: 107685, <https://doi.org/10.1016/j.ijfatigue.2023.107685>
9. Chen R Q, Chen G X, Liu X, Reliability prediction method for low-cycle fatigue life of compressor disks based on the fusion of simulation and zero-failure data. *Applied Sciences-Basel* 2022; 12(9): 4318, <https://doi.org/10.3390/app12094318>
10. Yu C Y, Guan Y L, Reliability synthesis and prediction for complex electromechanical system: A case study. *Frontiers in Energy Research* 2022; 10: 865252, <https://doi.org/10.3389/fenrg.2022.865252>
11. Denkena B, Dittrich M A, Keunecke L, Continuous modelling of machine tool failure durations for improved production scheduling. *Production Engineering* 2020; 14(2): 207-215, <https://doi.org/10.1007/s11740-020-00955-y>
12. Siju K C, Kumar M, Bayesian estimation of reliability using time-to-failure distribution of parametric degradation models. *Journal of*

- Statistical Computation and Simulation 2018; 88(9): 1717-1748, <https://doi.org/10.1080/00949655.2018.1445743>
13. Yalcinkaya M, Birgoren B, Confidence interval estimation of Weibull lower percentiles in small samples via Bayesian inference. *Journal of the European Ceramic Society* 2017; 37(8): 2983-2990, <https://doi.org/10.1016/j.jeurceramsoc.2017.02.050>
 14. Wang H L, Li J, Fu Y L, Zhang Z J, Reliability modeling and analysis of cycloid gear grinding machines based on the bootstrap-bayes method. *Journal of Advanced Mechanical Design, Systems, and Manufacturing* 2023; 17(3), <https://doi.org/10.1299/jamdsm.2023jamdsm0033>
 15. Maskura N, Lance F, A Family of Software Reliability Models with Bathtub-Shaped Fault Detection Rate. *International journal of reliability, quality and safety engineering* 2021; 28(5), <https://doi.org/10.1142/S0218539321500340>
 16. Huang L P, Gong Z L, Yue W H, Reliability simulation and prediction of mechanical equipment for maintenance. *Advanced Materials Research* 2010; 139-141: 1060-1063, <https://doi.org/10.4028/www.scientific.net/AMR.139-141.1060>
 17. Hoseinie S H, Behzad G, Uday K, Monte carlo reliability simulation of water system of longwall shearer machine. *International Journal of Reliability, Quality and Safety Engineering* 2013; 20(6), <https://doi.org/10.1142/S021853931350023X>
 18. Li C, Liu R X, Pan F K, Simulation of reliability prediction based on multiple factors for spinning machine. *Autex Research Journal* 2020; 20(1): 17-23, <https://doi.org/10.2478/aut-2019-0009>
 19. Xiao N C, Zuo M J, Zhou C N, A new adaptive sequential sampling method to construct surrogate models for efficient reliability analysis. *Reliability Engineering & System Safety* 2018; 169: 330-338, <https://doi.org/10.1016/j.ress.2017.09.008>
 20. Sun Z L, Wang J, Li R, LIF: A new Kriging based learning function and its application to structural reliability analysis. *Reliability Engineering & System Safety* 2017; 157: 152-165, <https://doi.org/10.1016/j.ress.2016.09.003>
 21. Mouzakitis A, Classification of fault diagnosis methods for control systems. *Measurement & Control* 2013; 46(10): 303-308, <https://doi.org/10.1177/0020294013510471>
 22. Tang S N, Yuan S Q, Zhu Y, Deep learning-based intelligent fault diagnosis methods toward rotating machinery. *Ieee Access* 2020; 8: 9335-9346, <https://doi.org/10.1109/ACCESS.2019.2963092>
 23. Yang P A, Yang J, Wang J L, Aero-engine gear fault diagnosis based on deep learning. *Journal of Vibration, Measurement and Diagnosis* 2022; 42(6): 1062-1067, <https://doi.org/10.16450/j.cnki.issn.1004-6801.2022.06.002>
 24. Mathur A, Kumar P, Harsha S P, Performance evaluation of three signal decomposition methods for bearing fault detection and classification. *Proceedings of the Institution of Mechanical Engineers Part K-Journal of Multi-Body Dynamics* 2023; 237(1): 114-130, <https://doi.org/10.1177/14644193221136661>
 25. Talhaoui H, Ameid T, Aissa O, Wavelet packet and fuzzy logic theory for automatic fault detection in induction motor. *Soft Computing* 2022; 26(21): 11935-11949, <https://doi.org/10.1007/s00500-022-07028-5>
 26. Lundgren A, Jung D, Data-driven fault diagnosis analysis and open-set classification of time-series data. *Control Engineering Practice* 2022; 121: 105006, <https://doi.org/10.1016/j.conengprac.2021.105006>
 27. Wang H L, Fang K, Li J, Xi C F, Analysis and experimental study on vibration characteristics of the RV reducer. *Advances in Mechanical Engineering* 2023; 15(6), <https://doi.org/10.1177/16878132231181328>
 28. Zhang J, Li N Z, Wei X J, Performance degradation analysis of reliability growth of airborne power supply based on logistic regression. *Journal of Physics: Conference Series* 2020; 1629(1), <https://doi.org/10.1088/1742-6596/1629/1/012029>
 29. Wang P, Li W B, Thermal and structural coupling finite element analysis and simulation of high-speed grinding electric spindle. *Mechanical Design and Manufacturing* 2016; 12: 146-149, <https://doi.org/10.3969/j.issn.1001-3997.2016.12.040>
 30. Zhao H X, Yang Z J, Chen C H, Optimization design of step stress accelerated degradation test for motorized spindle based on D-s optimality. *Applied Sciences-Basel* 2021; 11(9): 3832, <https://doi.org/10.3390/app11093832>
 31. Park M, Rhee S, A study on life evaluation & prediction of railway vehicle contactor based on accelerated life test data. *Journal of Mechanical Science and Technology* 2018; 32(10): 4621-4628, <https://doi.org/10.1007/s12206-018-0909-y>
 32. Huang Z G, Wang S H, Wang J J, Research on comprehensive evaluation method of CNC machine tools based on RAMS. *Journal of Mechanical Engineering* 2022; 58(9): 218-230, <https://doi.org/10.3901/JME.2022.09.218>